

# ELECTRONIC SUPPLEMENTARY INFORMATION

## Effects of deposited Pt particles on the reducibility of CeO<sub>2</sub>(111)

Albert Bruix,<sup>1</sup> Annapaola Migani,<sup>1</sup> Georgi N. Vayssilov,<sup>2</sup> Konstantin M. Neyman,<sup>\*,1,3</sup>  
Jörg Libuda<sup>4,5</sup> and Francesc Illas<sup>\*,1</sup>

<sup>1</sup> *Departament de Química Física & Institut de Química Teòrica i Computacional (IQTCUB), Universitat de Barcelona, C/ Martí i Franquès 1, 08028 Barcelona, Spain*

<sup>2</sup> *Faculty of Chemistry, University of Sofia, 1126 Sofia, Bulgaria*

<sup>3</sup> *Institució Catalana de Recerca i Estudis Avançats (ICREA), 08010 Barcelona, Spain*

<sup>4</sup> *Lehrstuhl für Physikalische Chemie II, Friedrich-Alexander-Universität Erlangen-Nürnberg, Egerlandstraße 3, D-91058 Erlangen, Germany*

<sup>5</sup> *Erlangen Catalysis Resource Center, Friedrich-Alexander-Universität Erlangen-Nürnberg, Egerlandstraße 3, D-91058 Erlangen, Germany*

---

\* Corresponding authors. E-mail: konstantin.neyman@icrea.es and francesc.illas@ub.edu

**Table S1: Extended Table 4.** Calculated oxygen vacancy formation energies  $E_f^{\text{O}_{\text{vac}}}$  in four different positions (Roman numbers) of the  $\text{Pt}_8/\text{CeO}_2$  system. For a given vacancy position (I to IV) different solutions for the electronic structure are denoted by a superindex (i.e. different number of total unpaired electrons or location and amount of  $\text{Ce}^{3+}$  centers).  $|\mu|_{\text{av}} \text{Ce}^{3+}$  and  $|\mu_{\text{T}}| \text{Pt}_8$  correspond to the average magnitude on the  $\text{Ce}^{3+}$  cations and the total magnitude of the  $\text{Pt}_8$  cluster, respectively, and  $q(\text{Pt}_8)$  is the Bader charge of the  $\text{Pt}_8$  cluster.

Model	Vacancy	# $\text{Ce}^{3+}$	$ \mu _{\text{av}} \text{Ce}^{3+}$ ( $\mu_{\text{B}}$ )	$ \mu_{\text{T}}  \text{Pt}_8$ ( $\mu_{\text{B}}$ )	$q(\text{Pt}_8)$	$E_f(\text{O}_{\text{vac}})$ (eV)
Opt	I <sup>1</sup>	4	0.93	0.02	0.53	2.73
Opt	I <sup>2</sup>	4	0.94	1.50	0.56	2.91
Opt	I <sup>3</sup>	4	0.93	0.05	0.53	2.76
Opt	II <sup>1</sup>	3	0.81	0.36	0.01	2.46
Opt	II <sup>2</sup>	3	0.87	1.11	0.09	2.48
Opt	II <sup>3</sup>	3	0.90	2.37	0.17	2.83
Opt	II <sup>4</sup>	4	0.74	0.94	0.16	2.75
Opt	II <sup>5</sup>	4	0.72	0.79	0.14	2.74
Opt	III <sup>1</sup>	4	0.83	0.33	0.48	2.92
Opt	IV <sup>1</sup>	5	0.85	0.25	0.76	2.53
Opt	IV <sup>2</sup>	5	0.79	0.15	0.65	2.59
Opt	IV <sup>3</sup>	4	0.90	0.10	0.63	2.62
Exp	II <sup>1</sup>	2	0.91	0.06	-0.08	2.34
Exp	IV <sup>1</sup>	3	0.94	0.73	0.42	2.70

**Table S2:** Energy ( $E_{\text{spill}}$ ) of reverse spillover of an oxygen atom from the  $\text{CeO}_2$  surface to the supported  $\text{Pt}_8$  cluster at the most stable positions of the vacancy  $\text{O}_{\text{vac}}$  and adsorbed atom  $\text{O}_{\text{ads}}$ .  $|\mu|_{\text{av}} \text{Ce}^{3+}$  and  $|\mu_{\text{T}}| \text{Pt}_8$  correspond to the average magnitude on the  $\text{Ce}^{3+}$  cations and the total magnitude of the  $\text{Pt}_8$  cluster, respectively.  $q(\text{Pt}_8)$  is the Bader charge of the  $\text{Pt}_8$  cluster.

Model	$\text{O}_{\text{vac}}$	$\text{O}_{\text{ads}}$	$\#\text{Ce}^{3+}$	$ \mu _{\text{av}} \text{Ce}^{3+} (\mu_{\text{B}})$	$ \mu_{\text{T}}  \text{Pt}_8 (\mu_{\text{B}})$	$q(\text{Pt}_8)$	$E_{\text{spill}} (\text{eV})$
Opt	II	$\text{Pt}_2$	3	0.85	1.03	0.79	1.00
Opt	II	$\text{Pt}_3$	3	0.82	0.32	0.88	1.24
Opt	IV	$\text{Pt}_2$	4	0.89	1.24	1.34	1.25
Exp	II	$\text{Pt}_2$	3	0.82	0.93	0.82	1.00

**Table S3:** Energy ( $E_{\text{ads}}$ ) of oxygen adsorption computed with respect to  $1/2\text{O}_2$  at various  $\text{O}_{\text{ads}}$  positions of the  $\text{Pt}_8$  cluster supported on  $\text{CeO}_2(111)$ .  $|\mu|_{\text{av}} \text{Ce}^{3+}$  and  $|\mu_{\text{T}}| \text{Pt}_8$  correspond to the average magnitude on the  $\text{Ce}^{3+}$  cations and the total magnitude of the  $\text{Pt}_8$  cluster, respectively and  $q(\text{Pt}_8)$  is the Bader charge of the  $\text{Pt}_8$  cluster.

$\text{O}_{\text{ads}}$	$\#\text{Ce}^{3+}$	$ \mu _{\text{av}} \text{Ce}^{3+} (\mu_{\text{B}})$	$ \mu_{\text{T}}  \text{Pt}_8 (\mu_{\text{B}})$	$q(\text{Pt}_8)$	$E_{\text{ads}} (\text{eV})$
$\text{Pt}_3$	2	0.85	1.03	1.55	-1.16
$\text{Pt}_2$	2	0.93	1.38	1.43	-1.30

**Figure S1:** Top (left panels) and side (right panels) views of the most stable computed  $\text{Pt}_8/\text{CeO}_{2-x}(111)$  structures with an oxygen atom removed from different positions (I-IV) of the slab to the gas-phase. Red spheres – O, purple – Ce, blue – Pt, yellow and light blue – spin density.

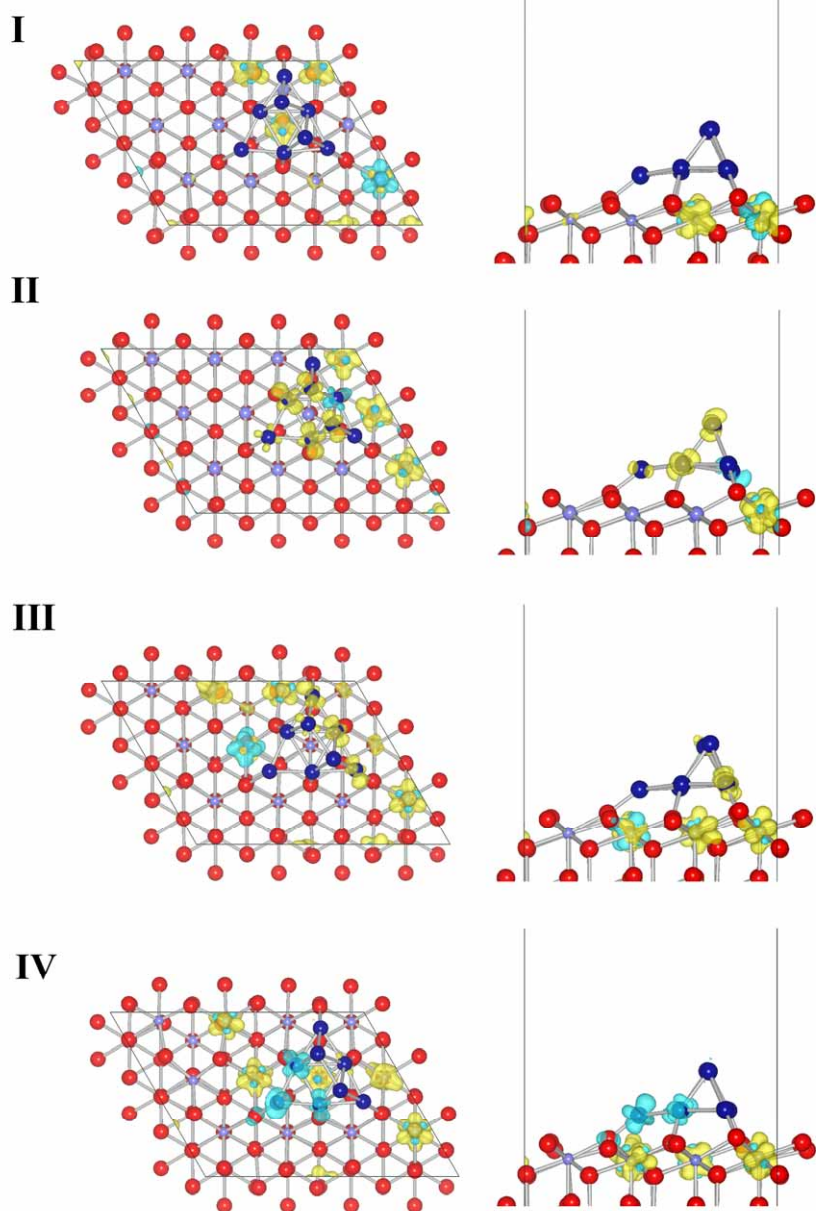
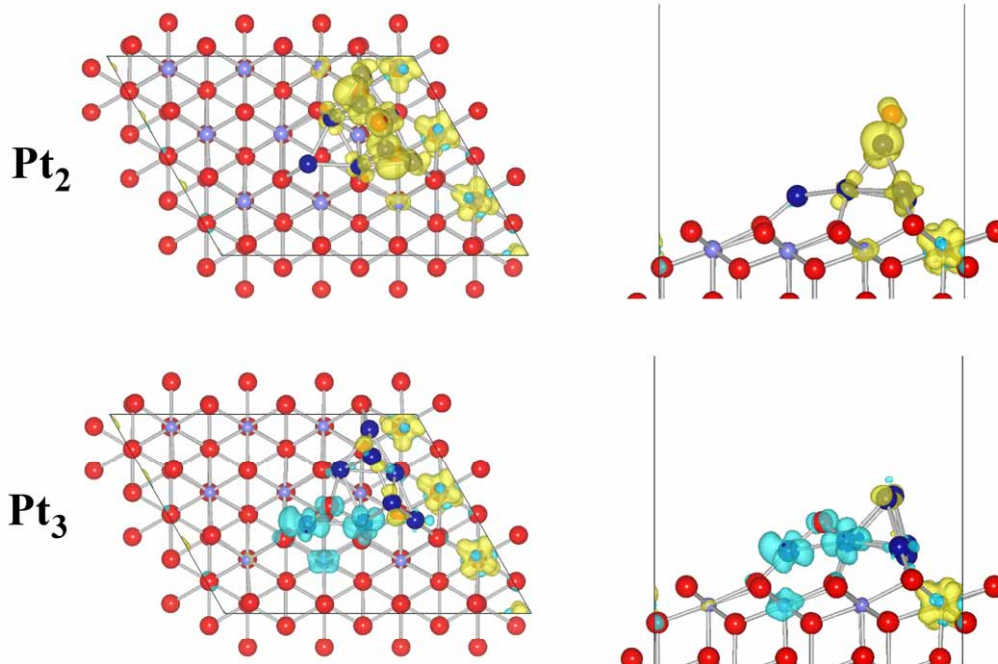


**Figure S2:** Top (left panels) and side (right panels) views of the most stable computed O-Pt<sub>8</sub>/CeO<sub>2-x</sub>(111) structures with an oxygen atom spilled-over from two different positions (II and IV) of the slab and adsorbed on different stable sites (Pt<sub>2</sub> and Pt<sub>3</sub>) of the Pt<sub>8</sub> particle. Red spheres – O, purple – Ce, blue – Pt, yellow and light blue – spin density.

**II:**



**IV:**

